

Simulation of the Burridge-Knopoff model of earthquakes with variable range stress transfer

Junchao Xia and Harvey Gould

Department of Physics, Clark University, Worcester, MA 01610

W. Klein

Department of Physics and Center for Computational Science, Boston University, Boston, MA 02215

J. B. Rundle

Department of Physics and Center for Computational Science and Engineering, University of California, Davis, CA 95616

Simple models of earthquake faults are important for understanding the mechanisms for their observed behavior, such as Gutenberg-Richter scaling and the relation between large and small events, which is the basis for various forecasting methods. Although cellular automaton models have been studied extensively in the long-range stress transfer limit, this limit has not been studied for the Burridge-Knopoff model, which includes more realistic friction forces and inertia. We find that the latter model with long-range stress transfer exhibits qualitatively different behavior than both the long-range cellular automaton models and the usual Burridge-Knopoff model with nearest neighbor springs, depending on the nature of the velocity-weakening friction force. This results have important implications for our understanding of earthquakes and other driven dissipative systems.

PACS numbers: 91.30.Px, 02.60.Cb, 05.20.-y, 05.45.-a

Earthquake faults are examples of driven dissipative systems [1]. Models of fault systems are important for understanding scaling laws, the occurrence of characteristic events, and the relation between small and large earthquakes [1, 2, 3]. In addition to the benefits that would result from understanding earthquake faults, understanding driven dissipative systems is important in physics and related areas.

Simulations of the Burridge-Knopoff model [4] have led to much insight. The model consists of blocks connected by linear springs to their nearest neighbors with spring constant k_c . The blocks are also connected to a loader plate by linear springs with spring constant k_L , and rest on a surface with a nonlinear velocity-weakening stick-slip friction force that depends on a parameter α which controls how quickly the friction force decreases as the velocity is increased and determines the amount of stress dissipated in an event. The model was studied numerically in one dimension [4] and more recently [5, 6, 7].

An earthquake event is defined as a cluster of blocks that move due to the initial slip of a single block. The moment of an event is $\propto \sum_j u_j$, where the sum is over all the blocks in an event and u_j is the net displacement of block j . The main result of prior studies [4, 5, 6] is that the moment distribution, $P(M)$, scales as M^{-b} for small localized events with an exponent $b \approx 2$ for $\alpha > 1$. Large events show a pronounced peak in $P(M)$ indicating a significant presence of characteristic or system-wide events. In contrast, the number of earthquake events with s blocks, $P(s)$, does not show power law scaling. Note that the blocks are connected only to their nearest neighbors in the Burridge-Knopoff model studied in Refs. [4, 5, 6, 7].

In the cellular automaton (CA) versions of the

Burridge-Knopoff model [8, 9] with nearest-neighbor stress transfer, $P(s)$ does not exhibit power law scaling [10]. A generalization of the CA models with long-range stress transfer yields considerable differences with the nearest-neighbor CA models [11] and with the nearest-neighbor Burridge-Knopoff model. In particular, the long-range CA models run in a Gutenberg-Richter scaling mode and exhibit events of all sizes, consistent with the system being near a mean-field critical point [12, 13, 14, 15]. Quasi-periodic system-wide events are not observed, and $P(s)$ exhibits power law scaling. Small and medium size events can be interpreted as fluctuations about a free energy minimum [12, 14]. Large events drive the system out of “equilibrium” from which the system decays back to an equilibrium state [12]. We refer to this behavior as punctuated ergodicity, which also has been observed in the Southern California fault system [16].

Both the CA and nearest-neighbor Burridge-Knopoff models lack several elements that would make them more realistic representations of earthquake systems. In particular, the latter does not include long-range stress transfer, and the long-range CA models do not have inertia and more realistic friction laws.

In this letter we discuss the results of adding more realistic long-range stress transfer to the Burridge-Knopoff model. Our primary result is that the statistical properties of this generalized Burridge-Knopoff model depend not only on the range R of the stress transfer, but also on the characteristics of the friction force. For large velocity weakening, that is, large α (see Eq. (2)), the properties of the Burridge-Knopoff model are largely independent of R , although there are some characteristics of the model that differ from the nearest-neighbor ($R = 1$) model and

are reminiscent of the long-range CA models. For small α and large R , the results are identical to the long-range CA models.

The usual ($R = 1$) Burridge-Knopoff model in one dimension is governed by the equation of motion

$$m\ddot{x}_j = k_c(x_{j+1} - 2x_j + x_{j-1}) - k_L x_j - F(v + \dot{x}_j), \quad (1)$$

where x_j is the displacement of block j from its equilibrium position, v is the speed of the substrate moving to the left with a fixed loader plate, $F(\dot{x}) = F_0\phi(\dot{x}/\tilde{v})$ is the velocity-dependent friction force, \tilde{v} is a characteristic velocity, and m is the mass of a block.

As in Ref. [5] we introduce scaled variables $\tau = \omega_p t$, $\omega_p^2 = k_L/m$, and $u_j = (k_L/F_0)x_j$, and rewrite Eq. (1) as

$$\ddot{u}_j = \ell^2(u_{j+1} - 2u_j + u_{j-1}) - u_j - \phi(2\alpha\nu + 2\alpha\dot{u}_j), \quad (2)$$

with $2\alpha = \omega_p F_0/k_L\tilde{v}$, $\ell^2 = k_c/k_L$, and $\nu = vk_L/(\omega_p F_0)$; the dots now denote differentiation with respect to τ . The friction force is

$$\phi(y) = \begin{cases} (-\infty, 1], & y = 0 \\ \frac{1-\sigma}{1+|y|^\sigma}, & y > 0. \end{cases} \quad (3)$$

We generalize the Burridge-Knopoff model by assuming that a block is connected to R neighbors (in each direction) with spring constant k_c/R ; $R = 1$ corresponds to the usual Burridge-Knopoff model. We use the second- and fourth-order Runge-Kutta algorithms with time step $\Delta t = 0.001$ to solve Eq. (2), modified for arbitrary R , with the friction force given in Eq. (3). Both algorithms and other fourth-order algorithms give similar results.

A block is defined to be stuck if its speed is less than the parameter v_0 , its velocity is decreasing, and the stress (the force due to the springs coupled to it) is smaller than the maximum static friction force F_0 (taken to be unity). If a block is stuck, its velocity is set equal to zero, and the static friction force cancels the stress. A stuck block will accelerate if the stress is greater than F_0 ; in this case the friction force drops to the value $1 - \sigma$. An earthquake begins with the slip of a block and ends when all blocks become stuck. Blocks can become stuck and then slip again during an event. The results in this paper are for $\ell = 10$, $\sigma = 0.01$, $v_0 = 10^{-5}$, $N = 5000$ blocks, $R = 1, 100, 500, 1000$, $\alpha = 0.0, 0.5$, and 2.5 , and 10^6 events.

We initially set $\dot{u}_j = 0$ for all j and assign random displacements to all the blocks. We compute the force on all the blocks and update \dot{u}_j and u_j for all j . We continue these updates until all blocks become stuck. We then move the substrate (the loader plate is fixed) until the stress on one block exceeds unity. This stress loading mechanism is known as the “zero velocity limit” [6] and is equivalent to setting $\nu = 0$.

In Fig. 1 we plot $P(M)$ for various values of R and α . For $\alpha = 2.5$ and $R = 1$, $P(M) \sim M^{-b}$ with $b \approx 2$ as in Ref. [5]. For larger values of R , b remains ≈ 2 , but the scaling range decreases and the characteristic earthquakes ($M > 1$) become better defined. For $\alpha = 0.5$ and

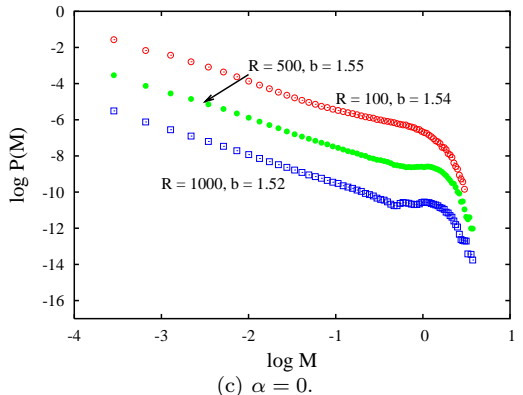
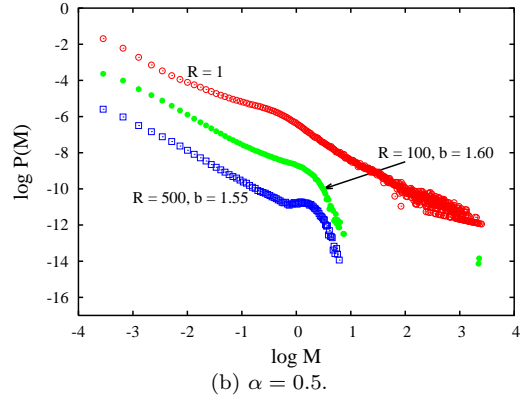
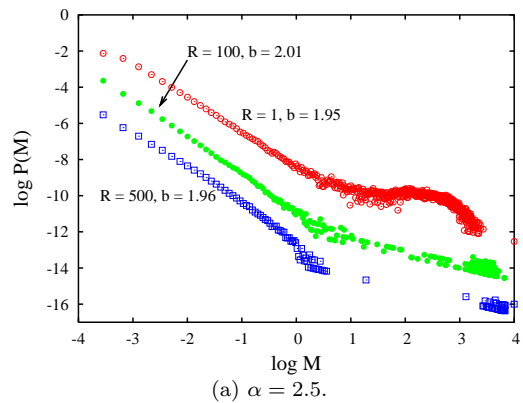


FIG. 1: Distribution of the moment M of the events $P(M)$. For $\alpha = 2.5$ and $R = 1$ the slope $b \approx 2$, consistent with Ref. [5]; b does not change significantly as R increases. For $\alpha = 0.5$ the scaling range becomes better defined as R increases and the slope converges to $b \approx 1.5$. For $\alpha = 0$, $b \approx 1.5$ for $R \gtrsim 100$; there is no power law behavior for $R = 1$ and small α . All plots have been displaced vertically for clarity.

$R \gtrsim 100$, b appears to approach 1.5 as R increases, and there are fewer characteristic earthquakes (see Fig. 1(b)). The results in Fig. 1(c) for $\alpha = 0$ are consistent with the long-range CA models [12, 13] for which $b = 3/2$. The distribution of events, $P(s)$, does not exhibit power law behavior for $R = 1$ and $\alpha = 2.5$, consistent with Ref. [5], but does so for larger R with $P(s) \sim s^{-b}$ and $b \approx 2$ (see Fig. 2). For small α , $b \approx 1.5$ for $R \gtrsim 100$.

We now consider the existence of ergodicity and determine the metric $\Omega_f(t)$ [17]. We take $f_j(t)$ to be a quantity

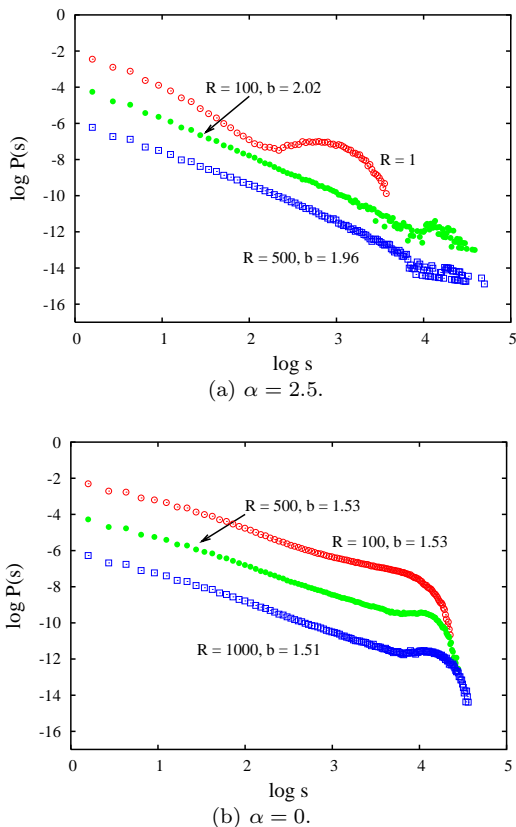


FIG. 2: Distribution of events of size s , $P(s)$. $P(s)$ does not exhibit power law behavior for $\alpha = 2.5$ and $R = 1$, but does so for larger R with $b \approx 2$. For $\alpha = 0$, $P(s) \sim s^{-b}$ with $b \approx 1.5$ for $R \gtrsim 100$. Note that s can exceed N because a block can fail multiple times during an event.

associated with block j and define

$$\bar{f}_j(t) = \frac{1}{t} \int_0^t f_j(t') dt' \quad (4)$$

$$\langle f(t) \rangle = \frac{1}{N} \sum_{j=1}^N f_j(t) \quad (5)$$

$$\Omega_f(t) = \frac{1}{N} \sum_{j=1}^N [\bar{f}_j(t) - \langle f(t) \rangle]^2. \quad (6)$$

If the system is ergodic, $\Omega_f(t) \propto 1/t$ [17]. The metric studied in the CA models is the stress metric. In Fig. 3 we show the inverse stress metric $\Omega_f^{-1}(t)$ for the Burridge-Knopoff model as a function of the number of times the substrate is moved (loading times). For $R = 1$ the system appears to be ergodic, unlike the short-range CA models [18]. For $\alpha = 2.5$, the system ceases to be ergodic for larger values of R . In contrast, for $\alpha = 0.5$ the system remains ergodic, and the slope of Ω_f^{-1} becomes larger as R increases. In particular, for $\alpha < 0.5$ and large R , the behavior of Ω_f is similar to the stress metric in the long-range CA models [19].

To understand this behavior, we plot the time series of the mean stress $\langle f \rangle$ per block just after an event for $R = 500$ (see Fig. 4). For $\alpha = 2.5$ $\langle f(t) \rangle$ is quasi-

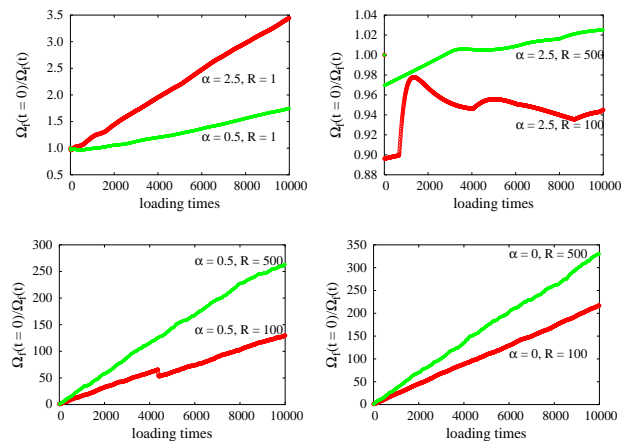


FIG. 3: The inverse stress metric versus the number of loading times. Note the different vertical scales. The system appears ergodic for $\alpha = 2.5$ and $R = 1$, but is nonergodic for larger values of R . For $\alpha = 0.5$, the slope of $\Omega_f^{-1}(t)$ becomes larger as R increases. For $\alpha = 0.5$ and $R = 100$, the system exhibits punctuated ergodicity similar to the behavior of the long-range CA model.

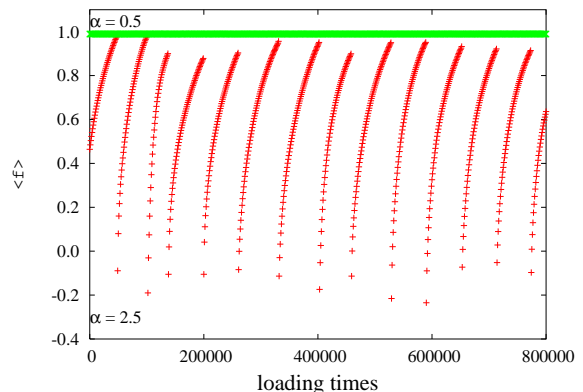


FIG. 4: The mean stress $\langle f \rangle$ as a function of the number of loading times for $R = 500$. Note the fluctuating behavior for $\alpha = 0.5$ and the quasi-periodic behavior for $\alpha = 2.5$.

periodic and ranges from ≈ -0.2 to almost 1.0 with a mean of ≈ 0.4 . That is, small earthquakes accumulate stress locally and characteristic earthquakes release the stress globally and quasi-periodically. The periodicity of characteristic earthquakes for $R = 1$ and $\alpha = 2.5$ was also analyzed in Ref. [7]. The distribution of characteristic earthquakes and other results [20] show that the periodicity becomes better defined as R is increased. The quasi-periodic behavior in Fig. 4 is reminiscent of the stress versus time curves observed in laboratory experiments with rocks [21]. In contrast, for $\alpha = 0.5$, $\langle f(t) \rangle$ fluctuates about ≈ 0.99 (see Fig. 4). The latter behavior is observed in long-range CA models [19].

Other statistical measures of the long-range Burridge-Knopoff model approach those of the long-range CA model. For example, the mean displacement (slip) of the blocks during an event, $\langle u \rangle$, as a function of s , the number of blocks in an event, is shown in Fig. 5. For large R the mean displacement is independent of the size of an event up to the largest events, as in the long-range

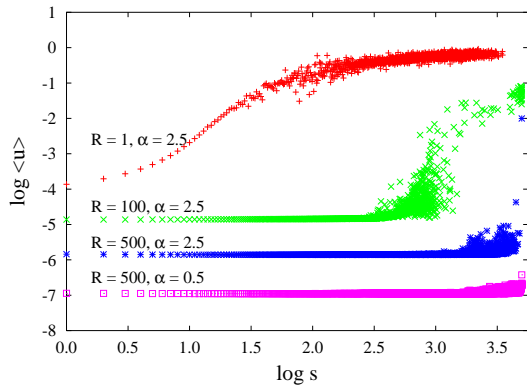


FIG. 5: The mean displacement $\langle u \rangle$ (slip) of the blocks as a function of the number of blocks s in an event. (Each block is counted once even if it fails multiple times.)

CA models. The range of events over which the mean slip is a constant increases with R .

In summary, we have found two possible scaling regimes, one of which ($\alpha \rightarrow 0$ and $R \gg 1$), is associated with an equilibrium spinodal critical point with an exponent $b = 3/2$ consistent with the long-range CA models [12, 13, 14, 15, 19]. The power law scaling of the moment for $\alpha = 2.5$ and $R = 1$ with $b \approx 2$ has been associated with critical behavior [5, 6]. This latter behavior and the ergodicity of the stress metric for this case suggests the presence of another critical point for short-range systems, but this interpretation needs more investigation. That is, the Burridge-Knopoff model appears to have two scaling regimes with qualitatively different behavior.

The apparent dependence of b on α suggests that larger

system sizes as well as longer run times should be investigated. However, because real faults are finite and the number of events observed is small, the α -dependence of b seen in the long-range Burridge-Knopoff model may accurately reflect the behavior of real faults.

For $\alpha = 2.5$ and large R , our results resemble those observed in laboratory experiments on rocks. As the range R is increased and α is made smaller, our results more closely resemble the long-range CA models. This wide range of behavior indicates that the physics of several models of earthquake faults [4, 5, 8, 9] can be obtained from the generalized Burridge-Knopoff model with the appropriate choice of R and α .

Our results imply that real earthquake faults and laboratory rocks can have different statistical distributions of events and different physical characteristics due to the details of the friction force as well as range of the stress transfer. This dependence means that we must develop ways of determining the friction force with considerably more accuracy if we want to understand the relation between physical processes and observed earthquake phenomena, and if we are to be able to predict earthquakes or even determine if they are predictable.

Acknowledgments

This work has been supported in part by DOE grant DE-FG02-95ER14498 (WK and JX) and DE-FG02-04ER15568 (JBR). The simulations were done at Clark with the partial support of NSF grant DBI-0320875.

-
- [1] J. B. Rundle, D. L. Turcotte, and W. Klein, editors, *Geo-Complexity and the Physics of Earthquakes*, American Geophysical Union, Washington, DC (2000).
 - [2] C. Scholz, *The Mechanics of Earthquakes and Faulting*, Cambridge University Press, Cambridge (1990).
 - [3] D. D. Bowman, G. Ouillon, C. Sammis, A. Sornette, and D. Sornette, *J. Geophys. Res.* **103**, 24359 (1998).
 - [4] R. Burridge and L. Knopoff, *Bull. Seismo. Soc. Amer.* **57**, 341 (1967).
 - [5] J. M. Carlson and J. S. Langer, *Phys. Rev. A* **40**, 6470 (1989).
 - [6] J. M. Carlson, J. S. Langer, B. E. Shaw, and C. Tang, *Phys. Rev. A* **44**, 884 (1991).
 - [7] T. Mori and H. Kawamura, *Phys. Rev. Lett.* **94**, 058501 (2005) and physics/0504218.
 - [8] J. B. Rundle and S. R. Brown, *J. Stat. Phys.* **65**, 403 (1991).
 - [9] Z. Olami, H. J. S. Feder, and K. Christensen, *Phys. Rev. Lett.* **68**, 1244 (1992).
 - [10] P. Grassberger, *Phys. Rev. E* **49**, 2436 (1994).
 - [11] J. B. Rundle and W. Klein, *J. Stat. Phys.* **72**, 405 (1993).
 - [12] See the article by Klein et al. in Ref. 1.
 - [13] G. Morein, J. B. Rundle, J. Xia, H. Gould, and W. Klein, manuscript in preparation. The authors consider a long-range CA model in which all blocks interact. As the noise level is decreased, a “bump” appears in the plot of the moment distribution, which suggests that there might be structure in the nonscaling curves of Fig. 1.
 - [14] J. B. Rundle, W. Klein, S. Gross, and D. L. Turcotte, *Phys. Rev. Lett.* **75**, 1658 (1995).
 - [15] W. Klein, J. B. Rundle, and C. Ferguson, *Phys. Rev. Lett.* **78**, 3793 (1997).
 - [16] K. F. Tiampo, J. B. Rundle, W. Klein, J. S. sa Martins, and C. D. Ferguson, *Phys. Rev. Lett.* **91**, 238501 (2003).
 - [17] D. Thirumalai and R. D. Mountain, *Phys. Rev. A* **42**, 4574 (1990) and D. Thirumalai and R. D. Mountain, *Phys. Rev. E* **47**, 479 (1993).
 - [18] J. B. Rundle, W. Klein, S. Gross, and D. L. Turcotte, *Phys. Rev. Lett.* **78**, 3798 (1997) and H.-J. Xu and D. Sornette, *Phys. Rev. Lett.* **78**, 3797 (1997).
 - [19] C. Ferguson, W. Klein, and J. B. Rundle, *Phys. Rev. E* **60**, 1359 (1999).
 - [20] J. Xia, H. Gould, W. Klein, and J. B. Rundle, manuscript in preparation.
 - [21] See the article by S. L. Karner and C. Marone in Ref. 1.